eLife

Reviewed Preprint
v1 • August 14, 2026
Not revised

For correspondence:
shaam.alabed@anu.edu.au
n.dehorter@uq.edu.au

* These authors contributed equally to the work and are listed alphabetically

Competing interests: No competing interests declared

Funding: See page 17

Reviewing editor: Laura A Bradfield, The University of Sydney, Australia

Reduced dorsal CA1 Activity Limits Retention of the Temporal Component of Declarative Memory in the *Cntnap2* Knockout Mouse Model of Autism

Elise C Rawlinson[1], Michael H McCullough[1,2], Azza Sellami[3,4], Aline Marighetto[3,4], A Shaam Al Abed[1,5,*], Nathalie Dehorter[1,5,*]

[1]Eccles Institute of Neuroscience, John Curtin School of Medical Research, The Australian National University, Canberra, Australia • [2]School of Computing, The Australian National University, Canberra, Australia • [3]Neurocentre Magendie, Physiopathologie de la plasticité neuronale, U1215, INSERM, Bordeaux, France • [4]Université de Bordeaux, Bordeaux, France • [5]The Queensland Brain Institute, The University of Queensland, Brisbane, Australia

eLife Assessment

This **valuable** study uses the Cntnap2 mouse model of autism to investigate how reduced activity in the dorsal CA1 region of the hippocampus contributes to impaired temporal binding and memory flexibility. The authors combined trace conditioning and radial maze assays with fibre photometry, optogenetic rescue, and brain-wide c-Fos mapping to provide **solid** evidence that dorsal CA1 hypoactivity limits the retention of temporally separated associations and biases learning towards less flexible strategies. The work advances understanding of hippocampal contributions to cognitive alterations associated with autism and will be of broad interest to researchers studying memory, hippocampal function, and neurodevelopmental disorders.

https://doi.org/10.7554/eLife.111851.1.sa3

Abstract

Growing evidence implicates the hippocampus in the pathophysiology of autism spectrum disorder, particularly in the domains of social interactions and cognition. Yet, the mechanisms driving hippocampal-dependent cognitive atypicalities in autism remain poorly defined. Here, we characterized how dysfunction of the CA1 subfield of the dorsal hippocampus drives critical components of declarative memory. Using trace fear conditioning in the *Cntnap2* knockout mouse model of autism, we found that capabilities to retain the association of temporally distant stimuli (*i.e.* temporal binding) were reduced relative to wildtype mice. Fiber photometry and optogenetic experiments demonstrated that reduced CA1 activity during temporal gaps underlies this impairment, linking CA1 dysfunction to a deficit of long-term memory retention in autism. Using a relational/declarative memory task, we also revealed a deficit in flexible spatial memory, and a preferential use of egocentric learning strategy. This unflexible learning strategy resulted from the imbalance between memory system activity, promoting frontostriatal-dependent procedural learning instead of dorsal CA1/hippocampus-dependent relational/declarative memory. Overall, this study establishes dorsal CA1 dysfunction as a circuit-level mechanism underlying cognitive inflexibility in autism, providing a neurobiological framework for hippocampal-dependent memory deficits in the condition.

Introduction

Autism spectrum disorder (ASD) is a lifelong neurodevelopmental disorder comprising difficulties in social behavior, atypical communication skills, and the presence of restricted or repetitive behaviors or interests (DSM-5 and Association American Psychiatric, 2013). Beyond these core features, individuals with ASD present with difficulties in cognitive domains which can impact daily functioning and adaptability. In particular, people with ASD present with atypicalities in episodic/declarative memory (Bal et al., 2015), the ability to recall specific events and experiences (i.e., *what happened, when, and where*). Yet, the underlying neurological mechanisms of declarative memory impairments in ASD remain to be fully elucidated.

While most research has focused on the dysregulation of the prefrontal cortex and the basal ganglia in ASD, recent studies have highlighted that hippocampal defects are key in the social domain of this phenotype (Banker et al., 2021). In addition, the hippocampus is known to play a critical role in declarative memory by forming temporally and spatially organized relational representations of past experiences, allowing flexible expression of memories (Eichenbaum, 2004). The CA1 subfield plays a key role in this relational process, by sustaining the ability to link temporally distant events, called temporal binding (Eichenbaum, 2014; Sellami et al., 2017). Difficulties in the binding of episodic memories have been proposed in autistic individuals, positing a selective weakness in hippocampus-dependent linking of items and contexts, while memory for items alone remains relatively spared (Bowler et al., 2011; Minor et al., 2023). In parallel with this relational hypothesis of memory defects, time estimation tasks in individuals with ASD have shown that disruptions in integrating temporal information affect the development of temporal relationships (Buonomano et al., 2023; Maister and Plaisted-Grant, 2011; Vogel et al., 2022). In this context, we hypothesized that CA1 activity underlying temporal processing and temporal linking is impaired in ASD, leading to declarative memory defects.

Here, we examined this hypothesis in the *Cntnap2* knockout (KO) mouse model of ASD, which exhibits autism-like phenotypes, including social behavior deficits (Peñagarikano et al., 2011; Peñagarikano and Geschwind, 2012) and hippocampal alterations, including CA1 circuit-level changes and impairments in spatial discrimination (Paterno et al., 2021). Animals were assessed in two behavioral paradigms: trace fear conditioning, a simple temporal binding-dependent memory task allowing the simultaneous recording of CA1 activity; and a radial maze task modeling the complexity of temporal binding-dependent relational/declarative memory. We demonstrate that *Cntnap2* KO mice present mistuned dCA1 activation and abnormal reorganization of memory systems during temporal binding-dependent memory formation.

Results

Cntnap2 KO mice demonstrate reduced temporal binding capability

We tested the temporal binding capabilities of the *Cntnap2* KO mouse model using the trace fear conditioning paradigm (TFC; Figure 1A), in which mice are required to memorize the association between a tone (Conditioned Stimulus) and a mild electric foot-shock (Unconditioned Stimulus), separated by a time interval called *Trace* (Sellami et al., 2017). In the first stage, i.e., the conditioning, independent groups of mice were exposed to three tone-shock pairings with a trace interval between 5 and 40 s (*i.e.* T5, T20, or T40; Figure 1A). All groups showed intact conditioning abilities, demonstrated by high and increasing freezing times (Blanchard et al., 1986) during the tones and traces periods (Figure 1B, Figure S1A). Elevated freezing during the pre-tone period may reflect fear generalization (Figure S1B, T20 vs. T40 (Sellami et al., 2017)). 24h later, the animals were re-exposed first to the conditioned *tone* in a neutral context (*i.e.* tone test) to assess 24h retention capacities of the tone-shock association. Retention was reflected in fear responses to the tone and trace compared with before and after the tone (*i.e.*, conditioned fear response in Figure 1B, % time freezing in Figure S1B). The animals were

then exposed to the conditioning *context* alone to evaluate contextual memory. As previously demonstrated (Al Abed et al., 2020b; Sellami et al., 2017), WT mice displayed efficient retention of the tone-shock association up to a 40-s trace interval (Figure 1C, Figure S1B), illustrated by strong and specific conditioned fear response to the tone in a neutral context (Figure 1C, Figure S1B). Interestingly, *Cntnap2* KO mice also displayed strong and specific freezing to the tone for up to a 20 s trace interval (Figure 1C, T20), but not for 40 s (Figure 1C, T40; Figure S1B, T40). These results were replicated in both control and KO littermates (Figure S1C). Altogether, these results indicate that *Cntnap2* KO mice exhibit reduced temporal binding capacity compared to WT mice, which compromises the 24h retention of the tone-shock association.

Because freezing is the absence of movement, the well-reported hyperlocomotion in *Cntnap2* KO mice ((Peñagarikano et al., 2011); Figure S1D) could represent a potential confounding factor. However, we observed comparable levels of resting time (Figure S1D, right panel) and similar freezing levels between WT and *Cntnap2* KO mice during acquisition, regardless of the trace interval (Figure S1A), as well as during memory tests under control conditions (Figure S1B; T5, T20, and T60). These findings indicate that locomotor activity alone cannot account for the observed differences in freezing performance. Taken together, our results demonstrate that *Cntnap2* KO mice exhibit reduced temporal binding capacity during conditioning, which does not affect acquisition but impairs the 24h retention of the tone-shock association.

Mistuning of dorsal CA1 activity during temporal binding in *Cntnap2* KO mice

Whilst alterations in item binding in ASD have already been reported, the underlying mechanisms have not been described (Minor et al., 2023). Because sustained activity of dCA1 neurons during time intervals between the stimuli is necessary for long-term retention of their association(Al Abed et al., 2020b; Sellami et al., 2017), we examined dCA1 activity during acquisition in *Cntnap2* KO mice. We recorded calcium transients during encoding and recall of trace fear conditioning, using fiber photometry in animals trained under a 20s or 40s-trace interval (Figure 1E). Both WT and *Cntnap2* KO mice implanted with an optic fiber could acquire the tone-shock association, reaching high levels of freezing after three tone-shock pairings (Figure 1F, Figure S1E). In both T20 and T40 conditions, regardless of genotype, tone frequency significantly decreased across tone presentations, suggesting neural adaptation to successive tone exposure (Figure S1F, G). *Cntnap2* KO mice trained under the 20s trace interval displayed no difference compared to WT in the frequency or amplitude of calcium transients during the tone and the trace interval (Figure S1F-H). In the 40s trace-conditioned group, while the frequency of the calcium transients did not differ between WT and C*ntnap2* KO mice throughout conditioning (Figure S1G), their amplitude was significantly reduced both during the presentation of the second tone and consistently across the three trace intervals in *Cntnap2* KO mice (Figure 1I). Overall, these results suggest a lack of synchronized neuronal activity during encoding, as previously reported (Simon and Wallace, 2016). During the tone test, as in Figure 1C, *Cntnap2* KO mice displayed appropriate retention of the tone-shock association when conditioned under a 20s-trace interval (Figure S1H, I) while the ones trained under a 40s-trace interval failed to express a fear response to the tone. This indicates impaired retention of trace fear memory and temporal binding ability, relative to WT mice (Figure 2I). The findings also suggest that sustained activity of dCA1 neurons during encoding of the three trace intervals, which is higher in WT than in *Cntnap2* KO mice, supports temporal binding and enables adequate retention of the association between the 40s-distant tone and shock despite their temporal separation, without affecting initial acquisition.

While the frequency of calcium transients remained unchanged in both T20 and T40 (Figure S1F, G), the amplitude of the peaks was higher during tone presentation in *Cntnap2* KO mice conditioned under the 20s trace interval (Figure 2J). In contrast, transient amplitude was lower during both tone presentation and the subsequent trace period in *Cntnap2* KO mice compared to WT mice (Figure 2K). These results further support the idea that the reduction in temporal binding capacity in *Cntnap2* KO mice stems from a lack of sustained dCA1 activity during encoding and recall of the tone-shock association.

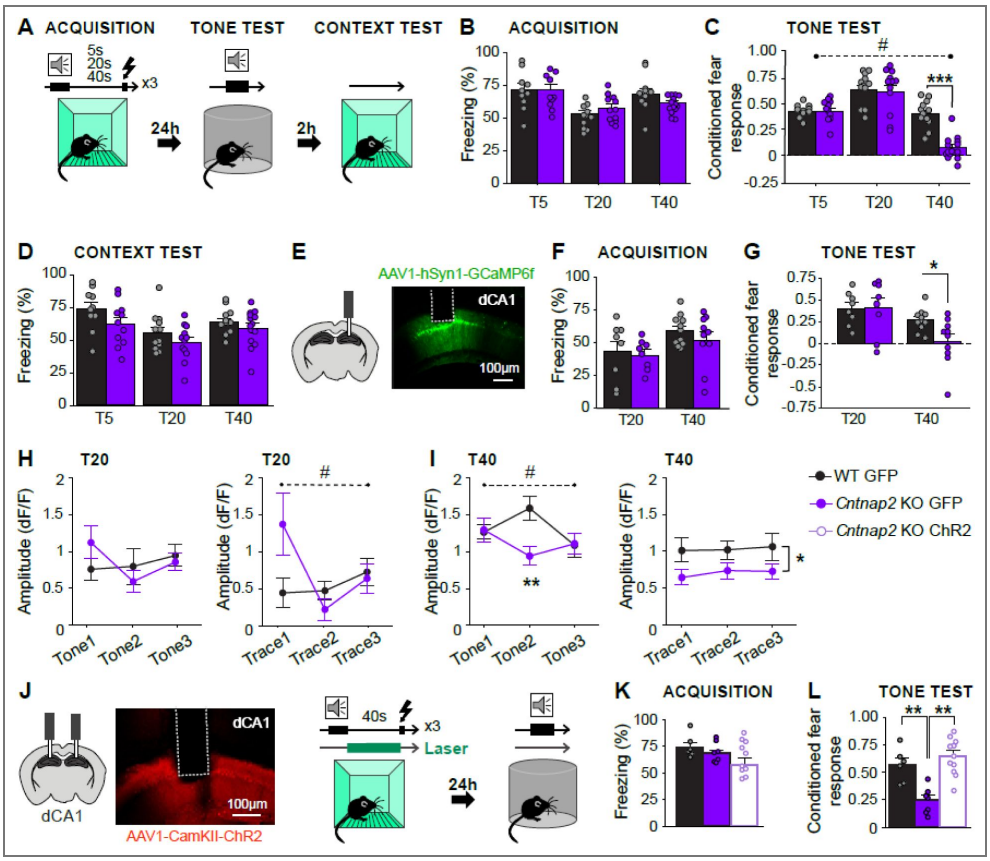

Figure 1. Reduced retention of temporal associations is associated with altered calcium responses during trace fear conditioning acquisition in *Cntnap2* KO mice

A. Experimental design: Trace Fear Conditioning includes a conditioning session in which mice have to associate a tone and a shock, separated by a time interval (trace). Independent groups of mice were trained with trace intervals of 5, 20, or 40 seconds. **B.** Freezing levels (percent) during the third tone of the conditioning session for WT (black) and *Cntnap2* KO (purple) groups, conditioned with distinct trace durations (T5: WT n=10; *Cntnap2* KO n=11; T20: WT n=12; *Cntnap2* KO n=11; T40: WT n=12; *Cntnap2* KO n=14). **C.** Conditioned fear response during the tone test (i.e., ratio of freezing before the tone compared to during the tone and the trace, see methods), 24h post-conditioning with distinct trace durations (Trace X Genotype interaction: $F_{2, 65}$=11.278; p<0.0001; T40: Genotype: $F_{2, 24}$=6.944; p=0.0163). **D.**Freezing levels in the conditioning context (context test) for WT (black) and *Cntnap2* KO (purple) groups, 24h post-conditioning. **E.** Fiber photometry. **Left** panel: scheme depicting the fiber optic implantation targeting the dorsal CA1 subfield of the hippocampus (dCA1). **Right** panel: Representative image of the optic fiber placement, in the pyramidal cell layer of the dCA1, scale: 100µm. Calcium activity was recorded using the calcium indicator GCaMP6f. **F.** Freezing levels (percent) during the third tone of the conditioning session for WT (black) and *Cntnap2* KO (purple) groups, conditioned with distinct trace durations (T20: WT n=8; *Cntnap2* KO n=8; T40: WT n=11; *Cntnap2* KO n=10). **G.** Conditioned fear response during the tone test (i.e., ratio of freezing before the tone compared to during the tone and the trace, see methods), 24h post-conditioning with distinct trace durations (T40: Genotype: $F_{1, 19}$=50.143; p<0.0001). **H. Left**: Peak amplitude of Ca^{2+} transients during the 3 tone presentations of the conditioning under a 20s trace-interval (ns). **Right**: Peak amplitude of Ca^{2+} transients during the 3 trace intervals of the conditioning under a 20s trace-interval (Genotype x Trace interaction: p=0.0476; WT n=8; KO n=8, trace 1: ns (p=0675)). **I. Left:** Peak amplitude of Ca^{2+} transients during the 3 tone presentations of the T40 conditioning session (Genotype x Tone interaction: p=0.0247; Tone: p=0.0053; WT n=11; KO n=10). **Right**: Peak amplitude of Ca^{2+} transients during the 3 trace intervals of the T40 conditioning session (Genotype: p=0.0408; WT n=11; KO n=10). **J.** Optogenetics: **Left** panel: scheme depicting the fiber optic implantations bilaterally targeting the dorsal CA1 subfield of the hippocampus (dCA1). **Right** panel: Representative image of the optic fiber placement, in the pyramidal cell layer of the dCA1, scale: 100µm. Pyramidal neurons activity was manipulated only during the trace interval using Channel Rhodopsin (ChR2). **K.** Freezing levels (percent) during the third tone of the conditioning session for GFP-injected WT (black, n=6), GFP-injected *Cntnap2* KO (purple, n=7), and ChR2-injected *Cntnap 2* KO (light purple/white, n=11) groups, conditioned with 40s trace duration. **G.** Conditioned fear response during the tone test (*i.e.*, ratio of freezing before the tone compared to during the tone and the trace, see methods), 24h post-conditioning with distinct trace durations (Groups: $F_{2, 21}$=15.576; p<0.0001; WT-GFP *vs* KO-GFP: p=0.0010; KO-GFP *vs* KO-ChR2: p<0.0001). Data shown at mean ± SEM. *: p<0.05; **: p<0.01; ***: p<0.001; * represents genotype effect. # represents genotype x variable interaction.

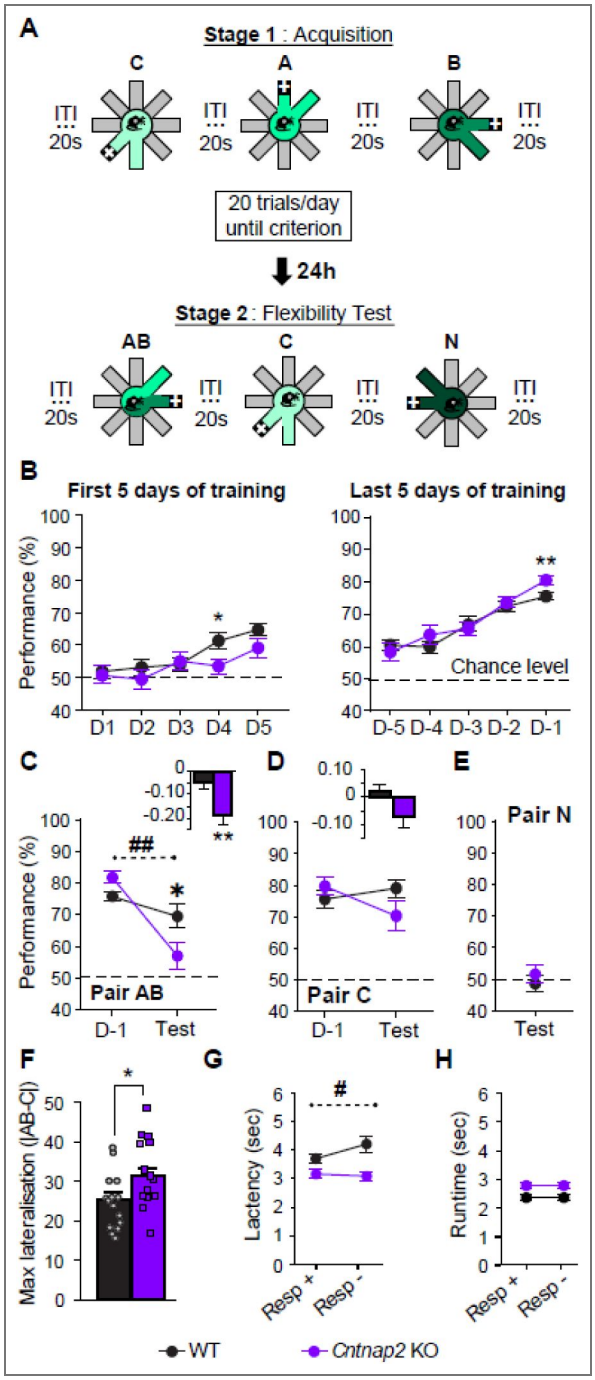

Figure 2. ***Cntnap2*** **KO mice display impaired relational/declarative memory.**

A. Experimental design: Relational/Declarative memory task. ITI: Inter-trial interval; +: represent reward location within each pair of arms. **B.** Average correct answers for WT (black; n = 15) and *Cntnap2* KO mice (purple; n = 14) for pairs A, B, and C during the 5 first days of acquisition (left panel; day (D); D4: Genotype: p=0.0149), and the last 5 days of acquisition (right panel; D-5: 5 days before they reach learning criterion; D-1: Genotype: p=0.0082). **C.** Comparison of the correct answers during the last day of training (D-1) averaged on pairs A and B, and during the flexibility test on the recombined pair AB (Genotype X Performance interaction: $F_{1,27}$=12.639, p=0.0014; Test, Genotype: p=0.0239). Inset: D-1 *vs.* Test performance index on pairs AB (Genotype: p=0.0022). **D.** Comparison of the correct answers on pair C during the last day of training (D-1) and the flexibility test. Inset: D-1 *vs*. Test performance index for Pair C. **E.** Average performance on the new pair N during the flexibility test. **F.** Maximum lateralization index during stage 1 (absolute value of the average performance between pairs A and B (left baited) minus Pair C (right baited); Genotype: p=0.0153). **G.** Average decision latencies for correct (+) and incorrect (–) answers throughout training (Genotype X Response interaction: $F_{1,31}$=7.960, p=0.0083). **H.** Average runtimes for correct (+) and incorrect (–) answers throughout training (Resp -, Genotype: p=0.0500). Dashed line illustrates chance level. Data shown at mean ± SEM. *: p<0.05; **: p<0.01; # shows genotype x performance interaction.

We previously demonstrated in WT mice that the activity of dCA1 principal neurons during the trace interval, but not during either the tone or the shock, is required for long-term retention, but not for encoding, of temporal associations (Sellami et al., 2017). To further confirm a causal link between sustained dCA1 activity during temporal gaps and 24h retention in *Cntnap2 KO*, we optogenetically activated principal neurons specifically during the 40s trace interval of the conditioning session, using ChannelRhodopsin (ChR2; Figure 1J), while leaving neuronal activity unaltered during the remainder of acquisition and the 24 h test. During the conditioning session, all groups displayed increased freezing across the three tone-shock pairings, indicative of efficient acquisition (Figure 1K, Figure S1J). 24h later, ChR2-expressing *Cntnap2* KO mice demonstrated a specific response to the tone and trace compared to before and after the tone, unlike GFP-expressing *Cntnap2* KO mice (Figure 1L, Figure S1K). These results demonstrate that dCA1 neuronal activity during trace intervals drives temporal binding in *Cntnap2* KO mice.

Egocentric learning and inflexible long-term memory in *Cntnap2* KO mice

Following the observation that *Cntnap2* KO mice present reduced dCA1 activity associated with temporal binding capabilities, we examined potential declarative memory atypicalities in declarative memory. We employed a radial maze task that models the complexity of temporal binding-dependent relational/declarative memory (Sellami et al., 2018). This task assesses the characteristic flexibility of R/DM expression, which relies on the dCA1-dependent ability to relate temporally distant events (Sellami et al., 2017).

To do so, the R/DM task is divided into two stages: an acquisition phase and a flexibility test (Figure 2A). In the acquisition stage, mice are trained daily to learn the food-reward location within 3 separate pairs of adjacent arms. After reaching the learning criterion (>75% correct choices of the rewarded arm), the flexibility of the memory learnt during acquisition is probed by recombining two pairs, without changing the position of the reward (pairs A and B recombined into pair AB; Figure 2A). Cumulative evidence shows that flexibility relies on hippocampus-dependent relational representation of separate experiences formed for each pair during the acquisition phase (Al Abed et al., 2020b; Mingaud et al., 2007; Sellami et al., 2017). To impose a temporal binding demand on relational memory acquisition, the presentation of each pair is separated by a 20s inter-trial interval (Sellami et al., 2017).

Both wild-type (WT) and *Cntnap2* KO mice were able to acquire the task (Figure 2B). *Cntnap2* KO mice tended to require more days to reach criterion (Average number of days: WT: 8.06, KO: 10.86, ns, data in Figure S2) and reached higher performance levels at the end of training (Figure 2B, right panel).

In the flexibility test, their performance dropped significantly between the last training session and the flexibility test (stage 2 of the R/DM task), and *Cntnap2* KO mice performed significantly worse than WT in the critical test of flexibility (Figure 2C - Recombined pair AB). In contrast, both groups performed similarly on the control pairs: the unchanged pair C, with high performance (Figure 2D), and the novel pair N, at chance levels (Figure 2E).

What could explain this lack of flexibility? We have previously shown that the flexibility component of R/DM depends on the learning strategy used during the acquisition stage: either allocentric spatial mapping (relational) or egocentric (procedural), the latter leading to lateralization. Indeed, when the use of spatial cues is impaired, as in cases of hippocampus damage or dysfunction, mice adopt a left-right egocentric strategy to memorize reward locations, leading to inflexible memory (Mingaud et al., 2007; Sellami et al., 2017). Therefore, the chance-level flexibility performance of *Cntnap2* KO mice suggests a bias towards a procedural learning strategy, in line with the well-documented prominence of behavioral inflexibility (Uddin et al., 2015) and the use of egocentric learning strategies (Brunner et al., 2015; Ring et al., 2018) in ASD. This was confirmed by analyzing lateralization during acquisition by comparing performance on left-baited pairs (pairs A and B), *vs.* right-baited pair C (Methods, Figure 2F). *Cntnap2* KO mice displayed significantly more lateralization than WT, meaning that they used an

egocentric/procedural strategy to learn the position of the food reward rather than using spatial mapping, as observed in WT mice. We found no significant correlation between the use of egocentric strategy and the number of days to reach criterion (Data in Figure S2). Notably, performance during Day 4 of acquisition in WT, but not in *Cntnap2* KO mice, was significantly negatively correlated with their use of lateralized strategy (r^2 = −0.518, p=0.0471). Together, this further confirms that *Cntnap2* KO mice employ a lateralized strategy to learn the task, which impacts both task performance (Figure 2B, day 4), and memory flexibility (Figure 2C).

Interestingly, *Cntnap2* KO mice had shorter decision times than WT (Figure 2G), consistent with the well-demonstrated impulsivity observed in ASD (DSM-5 and American Psychiatric Association, 2013). In addition, WT mice demonstrated a longer time to enter a non-baited arm than a baited arm, suggesting that they evaluate reward location before entering the arm, likely relying on deliberation and precise spatial representation. In contrast, *Cntnap2* KO mice showed similarly short latencies regardless of their choice, suggesting impulsive, automatic responses and impaired spatial representation of reward information. In addition, once a choice was made, their running time (from the central platform to the end of the arm) was longer than that of WT mice (Figure 2H), implying that the deliberative phase is shortened or absent in KO mice, while the slower run may reflect a compensatory adjustment following impulsive decisions.

Altogether, these findings show that *Cntnap2* KO mice exhibit impaired flexible memory expression, modeling a relational/declarative memory deficit associated with preferential use of an egocentric/procedural learning strategy.

Potential shift towards striatum-centered activities in *Cntnap2* KO mice

Each learning strategy is known to depend on partially distinct brain systems: hippocampus-dependent systems supporting allocentric spatial/relational learning, and striatum-based systems leading to egocentric/procedural learning (White and McDonald, 2002). To assess learning-induced activity in these different structures, we quantified the levels of the cellular activity marker cFos after day 3 of R/DM task acquisition in structures involved in memory (the dorsal hippocampus (dCA1, dCA2, dCA3, the dorsal dentate gyrus (dDG); the dorso-medial (DMS) and the dorso-lateral striatum (DLS); the prefrontal cortex (infralimbic (IL), prelimbic (PrL), and anterior cingular (ACC); Figure 3A).

As previously shown (Al Abed et al., 2020b; Sellami et al., 2017), we found a significant activation of dCA1 in trained WT mice compared to naïve WT mice, consistent with the use of an allocentric/spatial learning strategy (White and McDonald, 2002) (Figure 3B). In contrast, *Cntnap2* KO mice showed no learning-induced dCA1 activation together with hypoactivation of dCA3 in both naïve and trained groups compared to WT mice (Figure S2A). This reduced hippocampal activation likely underlies the deficit in temporal binding and spatial learning capabilities in this task. Moreover, *Cntnap2* KO mice displayed a significant training-induced activation of the DMS compared to their naïve controls, a pattern not observed in WT mice (Figure 3C). No other significant changes were detected in the DLS (Figure S2B) or in the prefrontal cortex regions (*i.e.*IL, PrL, ACC; Figure S2C). Together, this supports a shift toward DMS involvement in the egocentric learning strategy adopted by *Cntnap2* KO mice.

To further dissect the balance between memory systems, we analyzed the relative contribution of each structure within the total activation of the system (Figure 3D-E). After training, we found a disproportionate representation of the PFC and striatum relative to the hippocampus in *Cntnap2* KO mice compared to WT (Figure 3D).

Indeed, compared to WT naïve mice, WT trained mice exhibited an increase in the weight of the dCA1 in the network activity, likely supporting temporal binding and through ensuing relational organization of the 20s-distant pair presentations, the formation of flexible memory. In contrast, no such reorganization of network activity was observed in *Cntnap2* KO mice with training (Figure 3E). Differences in the relative contribution of individual substructures between trained WT

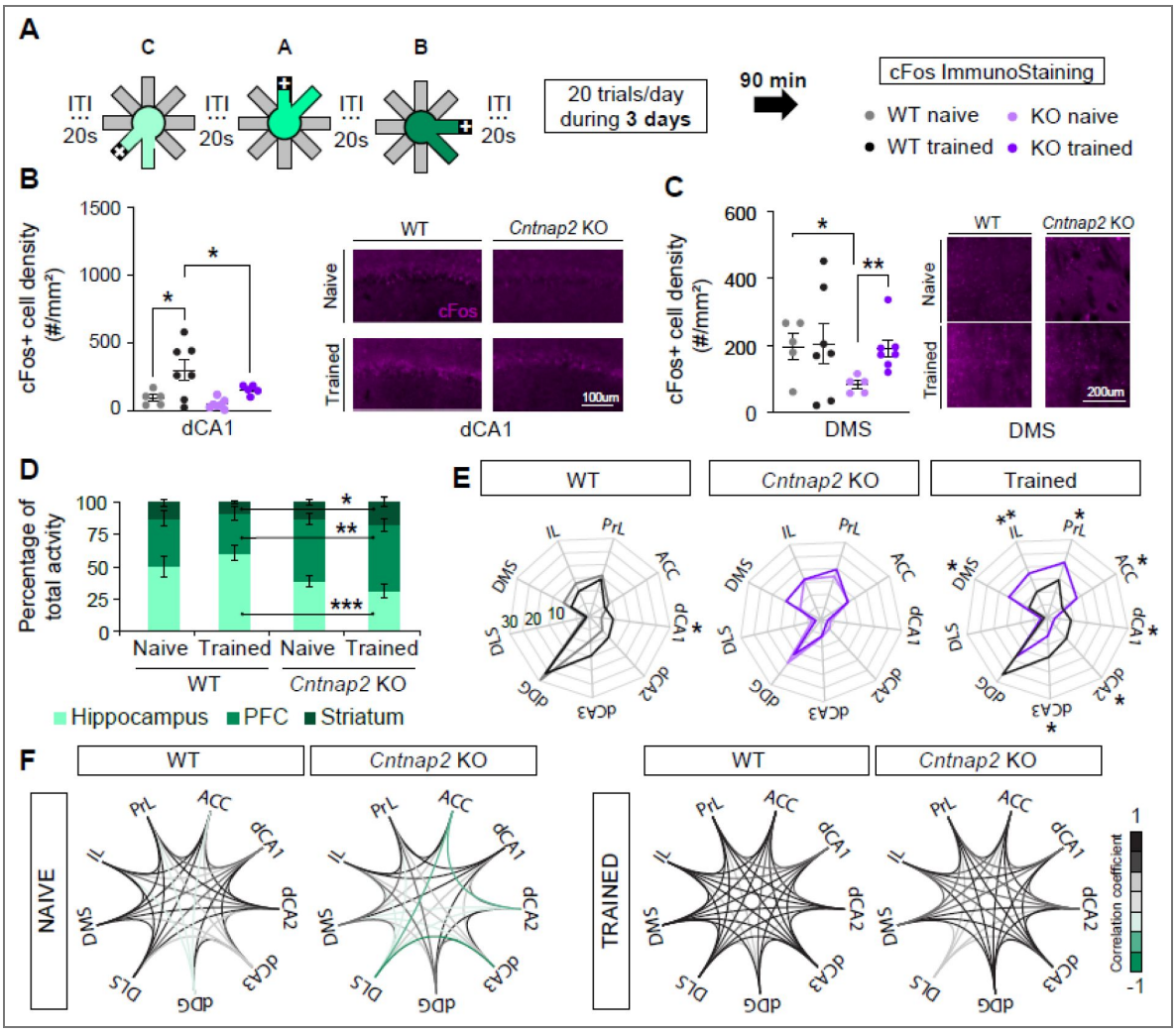

Figure 3. Learning-induced activity and functional connectivity in *Cntnap2* KO mice.

A. Experimental design: cFos levels were quantified 90min after the 3rd training session of the Relational/Declarative memory task. ITI: Inter-trial interval; + represents reward location within each pair of arms. **B.** number of cFos-positive neurons (cell density/mm^2) in the dorsal dCA1 (WT naïve vs Trained: p=0.0491; Trained WT vs. KO: p=0.0129) with representative images of the cFos staining (Magenta) in dCA1, scale: 100µm, for naïve (light colors) and trained (dark colors) WT (grey/black) and *Cntnap2* KO (purple) groups. **C.** number of cFos-positive neurons (cell density/mm^2) in the Dorso-Medial Striatum (DMS; Naive WT vs. KO: p=0.0189; KO Naïve vs Trained: p=0.0085) with representative images of the cFos staining (Magenta) in DMS, scale: 200µm. **D.** Percentage of total activity: activity of each structure over to the total activity measured (percentage; Trained WT vs. KO: Hippocampus: p=0.00023; PFC: p=0.00139; Striatum: p=0.02895). **E.** Percentage of total activity: activity each subfield within the total network, in WT mice (naïve vs trained, left panel; dCA1: p=0.0382), in *Cntnap2*KO mice (Naïve vs trained, middle panel), and in trained mice (WT vs *Cntnap2* KO mice, dCA1: p=0.0183; dCA2: p=0.0201; dCA3: p=0.0307; ACC: p=0.0378; DMS: p=0.0303; IL: p=0.0060; PrL: p=0.0476; right panel, same data as in left and middle panels). **F.** Pairwise between-structure correlation strength of cFos cell density. Data shown as mean ± SEM. *: p<0.05; **: p<0.01; # shows genotype x performance interaction.

and *Cntnap2* KO mice involved dCA1, dCA2, and dCA3, and favored the DMS, IL, and ACC. Overall, we observed compensatory activation of the frontal-striatal structures concomitant with hippocampal hypoactivation.

In addition to the learning-induced activity of individual structures, pairwise correlation of activity between structures enhances our understanding of network-wide synchronization. While naïve WT mice exhibited mainly positive correlations between the striatum, PFC, and hippocampus, with the exception of the dDG, which was negatively correlated with the PFC, naïve *Cntnap2* KO mice displayed predominantly negative correlations (Figure 3F).

This indicates that, at baseline, interstructural relationships are dysregulated in *Cntnap2* KO mice, potentially limiting the recruitment of a hippocampus-based learning strategy. Altogether, the analysis of learning-induced brain activity suggests a shift towards striatum-centered activity and connectivity in *Cntnap2* KO mice, likely promoting an egocentric learning strategy and resulting in inflexible memory.

Discussion

This study establishes a novel mechanistic framework that builds on prior reports of hippocampal alterations in *Cntnap2* KO mice (Paterno et al., 2021). It demonstrates that compromised CA1 hippocampal activity during encoding, disrupts temporal binding, which, by impairing the relational processing of temporally distant events, leads to deficits in retention of declarative memory. Moreover, hippocampal dysfunction in *Cntnap2* KO mice appears to shift learning away from hippocampus-dependent strategies, and toward egocentric strategies.

Interplay between hippocampus and striatum in memory deficits in *Cntnap2* KO mice

Atypicalities in declarative memory have been reported in ASD, with specific impairments in relating items (Minor et al., 2023). Here we demonstrate a reduction in dCA1-dependent temporal binding capacity in *Cntnap2* KO mice, which can contribute to the declarative memory impairment by disrupting the relational organization of temporally distant events. Indeed, in the trace fear conditioning experiments, *Cntnap2* KO mice showed efficient temporal binding with time intervals up to 20s, compared with 40s in WT mice, and this reduction was associated with a reduction of dCA1 activity during the encoding of the 40s-trace fear conditioning. Temporal integration of stimuli relies on hippocampal activity, in particular that of dCA1 (Buzsáki and Tingley, 2018; Chowdhury et al., 2005; Sellami et al., 2017; Tsien et al., 1996). Similarly, we found an impaired activation of the dCA1 in *Cntnap2* KO mice during the acquisition of the R/DM task (Figure 3B).

The lack of training-induced dCA1 activation likely prevents fine-tuned temporal integration of distant events, leading to flexibility deficits (Chang and Gold, 2003; Etchamendy et al., 2003; Mingaud et al., 2007; Sellami et al., 2017). Moreover, analysis of broader memory systems' activity during encoding revealed an aberrant recruitment of the DMS in the *Cntnap2* KO mice, along with an altered pair-wise correlation between activation of related brain regions (Figure 3F). While WT mice exhibited predominantly positive correlations, *Cntnap2* KO mice showed negative correlations among the DLS, prefrontal cortex and hippocampus. This pattern was also observed in naïve groups, suggesting that the bias towards lateralized learning strategy stems from baseline mistuning of functional connectivity between brain structures necessary for spatial learning in ASD.

This shift toward a striatum-centered system also implies a predominance of unconscious encoding, in which relations between items are acquired via stimulus–response associations, leading to inflexible, habit-like actions (Ferbinteanu, 2016). However, additional mechanisms may contribute to the phenotype. *Cntnap2* KO mice exhibit other neural and behavioral alterations (Peñagarikano et al., 2011), including epileptic seizures and hyperlocomotion, suggesting that CA1 hypoactivity is likely only one of several factors influencing performance.

Decoding spatial and temporal maps in the *Cntnap2* KO mouse model of autism

The CA1 region is recruited with other hippocampal areas to form and maintain spatial, temporal and social maps, which are mental relational representations of our environment (Barrientos and Tiznado, 2016). CA1 neurons contribute to encoding and recalling spatial information, enabling individuals to navigate and understand their surroundings. Specific "time cells" create a temporal framework that supports episodic memory, encoding the passage of time and the prediction of future events (Eichenbaum, 2014). Recent research also suggests that CA1 contributes to social cognition through so-called "social maps" which process and recall social information that is essential for effective social behavior and social dynamics (Zhang et al., 2022). Yet, little is known about how cognitive deficits evolve over time and their long-term effects in ASD. While the present study focused on dCA1 activation during acquisition to assess how dCA1 binds distinct stimuli into unified representations, future investigations directly examining the causal role of dCA1 activity in memory maintenance and retrieval (*e.g.* ArchT-mediated silencing during recall) will be essential for a comprehensive understanding of dCA1's role in memory processes in ASD, as well as for exploring how specific maps are formed and maintained in this condition.

The role of dCA1 in spatial representations has been profusely documented. Consistently, we recently demonstrated the central role of dCA1 in the maladaptive contextual encoding in post-traumatic stress disorder (PTSD), i.e., the degradation of declarative memory surrounding a highly stressful event (Al Abed et al., 2020a; Brewin, 2011; DSM-5 and American Psychiatric Association, 2013). Interestingly, growing evidence reports the propensity to develop PTSD in ASD (Al Abed et al., 2024; Rumball et al., 2020), suggesting that reduced dCA1 activation may impact cognition beyond everyday learning. Together, these studies further underscore the hippocampus as a promising target to alleviate ASD pathophysiology.

To obtain a deeper understanding of the hippocampus computation underlying memory formation, we analyzed the correlation between neuronal dynamics and behavioral outcomes within the fear memory test. Fiber photometry recordings in the dCA1 showed that whilst WT mice displayed sustained hippocampal activity during trace interval (Figure 1I), hippocampus-dependent memory systems were not similarly activated in the *Cntnap2* KO mice (Figure 3B, E). We found a marked decrease in the amplitude of calcium transients (Figure 1I). This profile was not observed when *Cntnap2* KO mice were trained within their capacity (*i.e.* 20 s trace interval; Figure 1H).

Overall, these results suggest that the deficits in temporal binding and declarative memory originate from reduced hippocampal neuronal synchronization and dynamics. In the same line, a recent study reported during contextual fear conditioning, that neurons allocated to the memory trace displayed freezing-specific activity compared to non-allocated neurons (Mocle et al., 2024). While our study design does not provide these details, the lack of active cells in the dCA1 during acquisition of the relational/declarative memory task could imply memory trace allocation to the striatum rather than the hippocampus (Rashid et al., 2016). Further experiments are needed to determine whether atypical engram allocation is linked to learning strategies in ASD.

Aged-like performance in *Cntnap2* KO mice suggests early cognitive decline

In this study, we demonstrate the disruption in hippocampal and CA1 functioning in the *Cntnap2* KO mice, a hallmark of memory defects observed during aging (Etchamendy et al., 2012; Leal and Yassa, 2015). Consistent with reports suggesting that people with autism are at risk of premature cognitive aging (Wang et al., 2024), we have found that young adult *Cntnap2* KO mice exhibit a memory profile similar to those of aged WT mice (Al Abed et al., 2020b; Marighetto et al., 2011; Sellami et al., 2017). Compared to young WT mice, both groups showed flexibility impairments in the relational/declarative radial maze task, and both exhibited a striatum-biased learning strategy. Yet, the underlying mechanisms driving these deficits remain unknown.

We previously demonstrated that dCA1 activity during the temporal gaps is necessary to link separate pairs into a relational/flexible memory (Al Abed et al., 2020b; Sellami et al., 2017) and that targeted dCA1 optogenetic activation during these intervals increases temporal binding capacity, rescuing relational/declarative memory formation. Given that CA1 neurons are less synchronized in ASD, targeted dCA1 activation could alleviate memory deficits. We propose that fine-tuning dCA1 activity may normalize memory system balance, offering a novel therapeutic approach for cognitive impairments in ASD. Further delineation of associated connectomes (Hollunder et al., 2024) could provide insights into targeted brain circuit therapies.

Autism is a highly heterogeneous condition, with individuals presenting a wide range of atypical cognitive abilities. Consequently, the extent and nature of memory deficits vary considerably across the spectrum. Research has yet to fully elucidate how these deficits manifest, particularly in relation to other cognitive domains such as attention, executive functioning, and language. Sex differences are another factor to consider (Van Wijngaarden-Cremers et al., 2014). While this study included both male and female mice, we did not observe sex-specific effects, suggesting that the behavioral and cognitive phenotypes examined in the *Cntnap2* KO mouse model are largely independent of sex. This is consistent with previous studies reporting no robust sex differences (Al Abed et al., 2024).

A better understanding of these individual differences is necessary to create more personalized and effective interventions. As such, further studies will have to assess these aspects in different models to fully comprehend the common cognitive mechanisms at play in autism.

Methods and material

Mice

3 to 5-month-old naive mice were collectively housed in standard Makrolon cages, in a temperature- and humidity-controlled room under a 12h light/dark cycle (lights on at 07:00), with *ad libitum* access to food and water. We used both males and females to minimize the number of mice produced in this study. *Cntnap2*$^{+/+}$ (WT) and *Cntnap2*$^{-/-}$ (KO) mice (Jackson ID: #017482 (Peñagarikano et al., 2011)) were non-littermate, though both lines were originally derived from breeders of the same colony and were used for behavior and histological analyses. To minimize potential differences between strains, we regularly inter-crossed the wildtype and *Cntnap2* KO colonies (*i.e.*, every year) to generate heterozygous mice. These heterozygotes were then bred to produce either WT or KO mice for experiments. Throughout the study, we used non-littermate mice originating from the same breeders. To ensure that observed differences between WT and *Cntnap2* KO were not influenced by this breeding strategy, we also assessed trace fear conditioning capacities in littermate mice and confirmed our findings using Het × Het breeding experiments (Figure S1).

All mice were bred in the same room, and maintained under identical husbandry and rearing conditions, including cage content, bedding, diet, and light/dark cycle. All experiments took place during the light phase. We replicated the behavioral experiments in two to four different batches. Every effort was made to minimize the number of animals used and their suffering. All procedures were conducted in accordance with the European Directive for the care and use of laboratory animals (2010-63-EU) and the animals care guidelines issued by the animal experimental committee of Bordeaux University (CCEA50, agreement number A33-063-099; authorization N°21248), and from the Australian National University Animal Experimentation Ethics Committee (protocol numbers A2018/66, A2020/26, A2021/43, and A2024/362).

Trace fear conditioning task (TFC)

Apparatus

Fear conditioning behavior was performed in a Plexiglas conditioning chamber (20 x 20 x 30 cm), in a brightness of 100 lux, given access to the different visual-spatial cues in the experimental room. The floor of the chamber consisted of stainless-steel rods connected to a shock generator

(Imetronic, Pessac, France).

Trace fear conditioning procedure

The box was cleaned with 70% ethanol before each trial. *During conditioning*, each animal received 3 pairings of a tone (70 dB, 1 kHz, 30 s) and a footshock (0.3 mA, 50 Hz, 1 s). The two stimuli were separated by a trace interval of 5, 20, or 40 s, depending on the group. Each tone-shock pairing was separated by a 1min-interval.

All mice were submitted 24 hours later to the *Tone retention test* during which they were re-exposed to the tone alone in a dark and modified chamber [circular opaque white chamber cleaned with a 1% acetic acid solution; 2min pre-tone, 2min tone and 2min post-tone]. A context test was also performed 2 hours later, during which mice were re-exposed to the conditioning chamber alone for 6 min.

Animals were continuously recorded for off-line scoring of freezing, by an experimenter ignorant of the experimental condition/group. Tone test was scored by 2 independent scorers. Freezing is defined as a lack of all movement except for respiratory-related movements. Acquisition of the TFC was measured by the progression of freezing during the tone across the 3 tone deliveries. 24h-retention of the trace association was measured during the tone test by the evolution of percentage of freezing time. Conditioned fear response to the tone was evaluated by calculating a normalized ratio between the tone and trace periods, *versus* outside these periods (i.e., Pre-Tone and Post-Tone): [(Tone+Trace)/2 - (pre-Tone+post-Tone)/2] / [(Tone+Trace)/2 + (pre-Tone+post-Tone)/2].

Radial-maze task of Relational/Declarative memory (R/DM)

Apparatus

We used an open 8-arm radial maze made of grey Plexiglas, automatized by videotracking (IMETRONIC – Pessac, France). The diameter of the central platform is 30 cm, and the arms are 55 cm long by 10 cm large. Each arm is equipped with a door at its entrance and a food-pellet delivery system at its end. The doors are individually controlled (raised up or dropped down) by the computerized system which also controls pellets availability in the food tray at the end of each arm individually, according to the task. The maze is placed in an empty room containing visual cues to enable spatial discrimination.

Behavioral Procedure

During the entire procedure, animals were submitted to one daily session. Prior to memory testing, animals were habituated to the apparatus over a period of two days during which animals were allowed to move freely in the radial maze. To complete the session, mice had to visit each arm until its end. Choice accuracy was measured as the percentage of correct responses for each pair.

Stage 1: Acquisition of 3-pair discriminations

The acquisition task consisted in learning the position of the food within the maze. Indeed, each animal was assigned three adjacent pairs of arms (pairs A, B and C). In each pair, only one arm was baited as a food reward. The experiment is designed in a way that the left arms of pairs A and B are baited while the right arm of pair C is. In each trial, mice were given access to a pair (either pairs A, B, or C). A choice was made when the subject reached the food well of an arm; this also closed the door of the non-chosen arm. The trial was finished as soon as the animal returned to the central platform. The subject was then confined to the central platform for 20s before the next discrimination trial began: this constituted the inter-pair interval (ITI). Each daily session consisted of 20 consecutive trials comprising alternate presentations of pairs A, B, and C according to a pseudo-random sequence. A mouse was considered to reach criterion when its overall choice accuracy was at or above 75% over two consecutive sessions given that performance in each of the three discrimination choices were at least 62% correct. The flexibility test task began the following day when criterion performance was reached. Lateralization index was quantified by using the

absolute value of the subtraction of the performance on the left-baited pairs vs. the right-baited pairs. Lat = |((Pair A + Pair B) /2) - Pair C|. We then used the maximum lateralization over 3 consecutive days.

Stage 2: Flexibility probe of DM

In the test task, the position of the food in the maze did not change, but characteristic flexibility of DM expression was assessed by changing the way of presenting the arms. Indeed, in place of the pairs A and B, a pair AB was submitted to the mouse. The AB pair consisted in the combination of the two adjacent arms of the pairs A and B. It was the critical test of flexibility. Two other pairs were used as control: the pair C that remained unchanged ("unchanged learnt control", and pair N (=new) made of the two arms non-used in acquisition ("unlearnt control").

Fiber photometry

Surgery

Mice were injected unilaterally 4 weeks before behavioral experiments with an Adeno-Associated Virus (AAV) GCaMP6f (AAV1-hsyn-jGCaMP6f-WPRE, Addgene). We used glass pipettes (tip diameter 25-35 µm) connected to a picospritzer (Parker Hannifin Corporation) into the right side of the dorsal CA1 of the hippocampus (0.1 µl/site; AP −1.8 mm; L +1.35 mm; DV −1.4 mm). Mice were then implanted with unilateral optic fiber implant (diameter: 200µm; numerical aperture: 0.39; flat tip; Neurophotometrics). Implants were fixed to the skull with Super-Bond dental cement (Sun Medical, Shiga, Japan). Mice were perfused after experiments to confirm correct placements of fibers. Viral injections targeted the pyramidal cell layer of the dCA1.

Recordings

Data were recorded throughout the entire fear conditioning paradigmusing a Neurophotometrics FP3002 system (Neurophotometrics, San Diego, CA). Briefly, 470 nm and 415 nm LED light was bandpass filtered, reflected by a dichroic mirror, and focused onto a multi-branch patch cord (Neurophotometrics, San Diego, CA) by a x20 objective lens. Alternating pulses of 470 and 415 nm light (~50 µW) were delivered at 60 Hz, and photometry signals were time-locked to behavior using a Bonsai workflow. Signals were analyzed using the Synaptech suite cloud service (MetaCell) and custom-made Python scripts (Code available at *https://github.com/elisecr/fiberphotometry_2024*). Through the Synaptech platform, 470 and 415 signals were deinterleaved. For all experiments, the exponential delay period (the first 10 seconds(Hon et al., 2025)) of the recording was removed. To correct for photobleaching, isosbestic (415nm) signals were fit to a biexponential curve to model the baseline signal with photobleaching. The fitted biexponential curve was then scaled to match the 470nm signal using non-negative robust linear regress and subtracted from the 470 trace to correct for baseline drift. Traces were then Z-scored.

Experimental traces

Z scored data were analyzed by custom python scripts to extract calcium fluorescence traces for each experiment. For the trace fear conditioning experiments, these data were aligned to files generated by the poly fear software (Imetronic, France) ".dat" files to align the beginning of the tone and shock events to the closest millisecond in the Z scored data. The timing of the tones and trace periods were extracted as described above to accurately align the data.

Peak finding

The threshold for peak analysis definition was set at 1.0. Peak analysis was conducted using a custom-built Python script to calculate peak frequency and amplitude. Code available at *https://github.com/elisecr/fiberphotometry-analysis*

Optogenetic Manipulation of dCA1

Surgery

Mice were injected bilaterally 5 weeks prior to behavioral experiments with an Adeno-Associated Virus (AAV) containing the excitatory opsin channelrhodopsin targeting the pyramidal cells of dCA1 (pAAV-CaMKIIa-hChR2(H134R)-mCherry (#26975), Addgene). We used glass pipettes (tip diameter 25-35 µm) connected to a picospritzer (Parker Hannifin Corporation) into the dorsal CA1 of the hippocampus (0.2 µl/site; AP −1.8 mm; L +1.3 mm; DV −1.4 mm and AP −2.5 mm; L +2 mm; DV −1.4 mm). Mice were then implanted with bilateral optic fiber implant (AP −1.8 mm; L +1.3 mm; DV −1.3 mm; diameter: 200µm; numerical aperture: 0.39; flat tip; Neurophotometrics). Implants were fixed to the skull with Super-Bond dental cement (Sun Medical, Shiga, Japan). Mice were perfused after experiments to confirm correct placements of fibers. Viral injections targeted the pyramidal cell layer of the dCA1. *Optogenetic manipulation during trace fear conditioning:* Mice were conditioned under a 40s trace interval condition, while dCA1 pyramidal neurons were activated during the 40 seconds of trace interval only. The light (≈3 mW per implanted fiber) was bilaterally conducted from the laser (Neurophotometrics, 450nm; 5 Hz; 5 ms laser on, 195 ms laser off) to the mice via two fiber-optic patch cords (diameter, 200 µm; Doric Lenses). The tone test was performed 24h later, mice were tethered to the patch chord, without optogenetic manipulation.

Open field

Mice were placed in a 38.5cm diameter circular arena and allowed free exploration for 5 minutes. These movements were recorded, and the mean velocity, distance travelled, and resting time were tracked and quantified using a custom MATLAB (Mathworks) code as in (Parkinson et al., 2024).

Immunohistochemistry

Naïve (homecage) and trained (90 min after the flexibility test on Day 3 for c-Fos analysis) animals were perfused transcardially with 0.01M phosphate buffered saline (PBS) to eliminate blood and extraneous material, followed by 4% paraformaldehyde (PFA). Brains were postfixed for 36h in PFA. Tissues were sectioned at 40 µm using a Leica 1000S vibratome and kept in a cryoprotective ethylene glycol solution at −20°C until processed for immunofluorescence. Sections were first washed and permeabilized in PBS-Triton 0.25%, then non-specific binding sites were blocked by immersing the tissue in 10% normal donkey serum, 2% bovine serum albumin in PBS-Triton 0.25% during 2h. Tissues were then stained using the primary antibodies overnight: mouse anti-c-Fos (1:1000; Santa Cruz). After 3x 15 min washes, we added anti-rabbit Alexa 488 (1:200; Life Technologies) secondary antibodies for 2h. After 3x 15 min washes slices were stained during 5 min with DAPI (5µM; Sigma), mounted on Livingstone slides then covered with Mowiol (Sigma) and coverslip (Thermofisher). c-Fos, staining from 2-3 slices par animals were imaged using a Nikon Axioscan confocal fluorescent microscope (20x objective). Stained sections of WT and mutant mice were imaged during the same imaging session. Immunofluorescence signals were quantified using the quPath software with routine particle analysis procedures (size= 30-500; circularity=0.30-1.00), to obtain cellular masks, divided by the area to obtain cell density per mm^2.

Statistics

Data are presented as mean ± SEM. Statistical analyses were performed using GraphPad prism or StatView software for 2-way ANOVA, followed by Bonferroni *post-hoc* test or Student's t test, when appropriate. Normality of the data was confirmed using the Kolmogorov–Smirnov test. Statistical significance was considered at $p<0.05$.

Data availability

Raw data provided in additional files contains the numerical data used to generate the figures. Code available at *https://github.com/elisecr/fiberphotometry_2024*.

Supporting figures

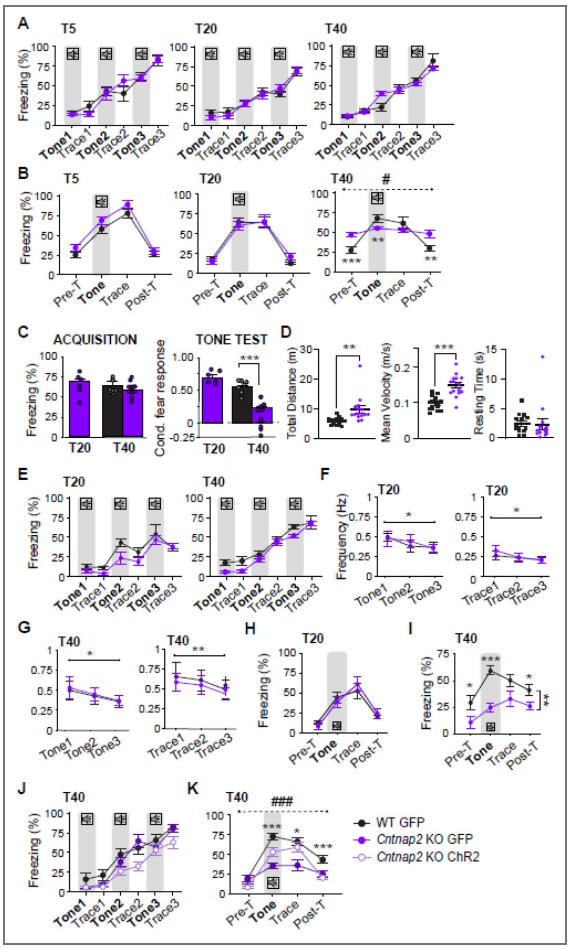

Supplementary Figure S1. Freezing levels and calcium peak frequencies during the fiber photometry recordings (Figure 1).

A. Freezing levels (percent) during the conditioning session for WT (black) and *Cntnap2* KO (purple) groups, conditioned with distinct trace durations (T5: 5s trace interval, T20: 20s trace interval; T40: 40s Trace interval). **B.** Freezing levels (percent time freezing) during the pre-tone, tone, trace and post-trace periods in the tone test for WT (black) and *Cntnap2* KO (purple) groups, 24h post-conditioning with distinct trace durations (T40: Pre-tone: p=0.001; Tone: p=0.0177; Trace: p=0.261; Post-Tone: p=0.0064; Genotype x Freezing interaction: $F_{3, 72}$=12.671; p<0.0001). **C. Left:** Freezing levels (percent) during the third tone of the conditioning session for littermate WT (black) and *Cntnap2* KO (purple) T20 and T40 groups, (T20: *Cntnap2* KO n=6; T40: WT n=8; *Cntnap2* KO n=12). **Right:** Conditioned fear response during the tone test for the littermate groups (i.e., ratio of freezing before the tone compared to during the tone and the trace, see methods), 24h post-conditioning with distinct trace durations (Trace in *Cntnap2* KO: p<0.0001; Genotype in T40: p<0.0001). **D.** Analysis of locomotion in an open field. **Left:** Total distance (m); genotype: p=0.046. **Middle:** Mean velocity (m/s); genotype: p<0.0001. **Right:** Resting time (s); genotype: ns; n= 14 WT, 15 *Cntnap2* KO. **E.** Fiber photometry: Freezing levels (percent) during acquisition of trace fear conditioning for WT (black) and *Cntnap2* KO (purple) groups, conditioned with a 20s (T20, n=8 WT and n=8 *Cntnap2* KO, left panel) or a 40s trace interval (T40, n=11 WT and n=10 *Cntnap2* KO, right panel). **F. Left:** Peak frequency of Ca^{2+} transients during the 3 tone presentations of the T20 conditioning (tone effect: p=0.0176). **Right:** peak frequency of Ca^{2+} transients during the 3 trace intervals of the T20 conditioning (trace effect: p=0.0287). **G. Left:** peak frequency of Ca^{2+} transients during the 3 tone presentations of the T40 conditioning (tone effect: p=0.0018). **Right:** peak frequency of Ca^{2+} transients during the 3 trace intervals of the T40 conditioning (trace effect: p=0.0229). **H.** Freezing levels (percent) during the tone test of the fiber photometry (T20) for WT (black) and *Cntnap2* KO (purple) groups, 24h post-T20 conditioning (ns; WT n=8; KO n=8). **I.** Freezing levels (percent) during the tone test of the fiber photometry (T40) for WT (black) and *Cntnap2* KO (purple) groups, 24h post-conditioning (Genotype: p=0.0009; PreTone: p=0.0258; Tone: p<0.0001; Post-Tone: p=0.0177; WT n=11; KO n=10). **J.** Optogenetic: Freezing levels (percent) during acquisition for GFP-injected WT (black; n=6), GFP-injected *Cntnap2* KO (purple; n=7), and ChR2-injected *Cntnap2* KO (light purple, white circles n=11) groups, conditioned with a 40s trace interval (Group: ns). **K.** Freezing levels (percent) during the tone test for GFP-injected WT (black; n=6), GFP-injected *Cntnap2* KO (purple; n=7) and ChR2-injected *Cntnap2* KO (light purple white circles n=11) groups, 24h post-T40 conditioning (Group x freezing: $F_{6, 63}$ = 5.656; p<0.0001; Tone: p=0.0009; Trace: p=0.0224; Post-T: 0.0004).

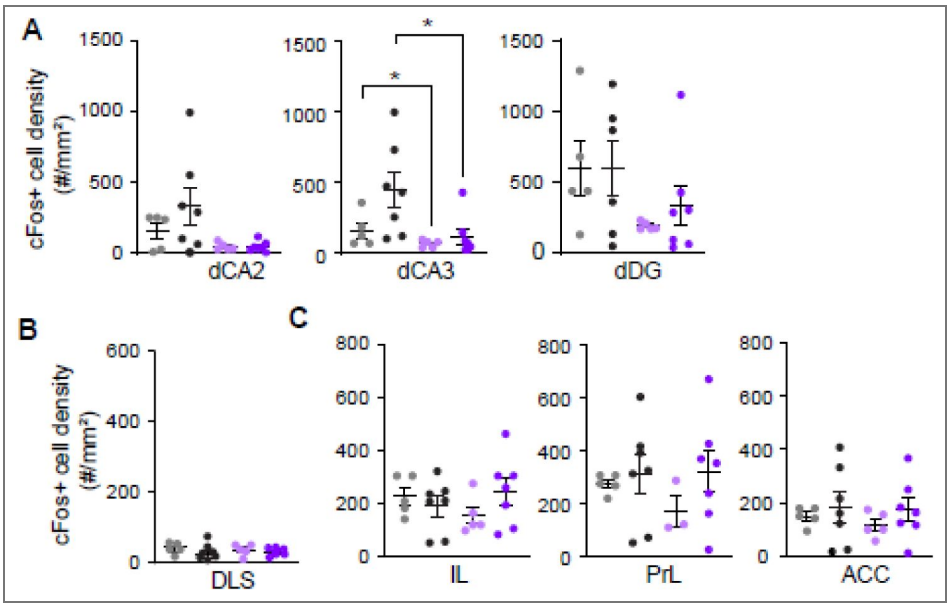

Supplementary Figure S2. cFos density in the hippocampus, striatum, and prefrontal cortex.

A. Number of cFos-positive neurons (cell density/mm^2) in the dorsal hippocampus subfields: dCA2, dCA3 (Naive WT vs. KO: p=0.0400; Trained WT vs. KO: p=0.0454), dDG for naïve (light colors) and trained (dark colors) WT (grey/black) and *Cntnap2* KO (purple) groups. **B.** Number of cFos-positive neurons (cell density/mm^2) in the Dorso-Lateral Striatum (DLS; ns). **C.** Number of cFos-positive neurons (cell density/mm^2) in the prefrontal cortex: Infra-Limbic, Pre-Limbic, Anterior Cingular Cortex (PFC, IL, PrL, ACC, respectively). Data shown at mean ± SEM. *: p<0.05.

Acknowledgements

We thank all the personnel of The Australian Phenomics Facility and of The Neurocentre Magendie involved in mouse care.

Additional information

Funding

Australian National University Futures scheme, NHMRC Ideas Grant 2019416, Centre National pour la recherche scientifique (CNRS), Bordeaux University, L'institut national de la santé et de la recherche médicale (INSERM), the John Curtin School of Medical Research.

Author contributions

Conceptualization: ASA;

Methodology: ASA, ND, AM, MHM;

Investigation: ASA, ECR

Writing—original draft: ASA, ND

Writing—review & editing: ND, ASA, AM, ECR, MHM

Funding

Funder	Grant reference number	Author
Australian National University (ANU)		Elise Caitlin Rawlinson Michael H McCullough Alice Shaam Shaam Al-Abed Nathalie Dehorter
Centre National de la Recherche Scientifique (CNRS)		Aline Marighetto
Institut National de la Santé et de la Recherche Médicale (Inserm)		Aline Marighetto Azza Sellami

Author ORCID iDs

Michael H McCullough: https://orcid.org/0000-0001-6572-565X
A Shaam Al Abed: https://orcid.org/0000-0002-6091-810X

Additional files

Raw Data

References

Al Abed AS, Allen TV, Ahmed NY, Sellami A, Sontani Y, Rawlinson EC, Marighetto A, Desmedt A, Dehorter N (2024) Parvalbumin interneuron activity in autism underlies susceptibility to PTSD-like memory formation. *iScience* **27**:109747 https://doi.org/10.1016/j.isci.2024.109747 | PubMed

Al Abed AS, Ducourneau E-G, Bouarab C, Sellami A, Marighetto A, Desmedt A (2020a) Preventing and treating PTSD-like memory by trauma contextualization. *Nature Communications* 1-9 https://doi.org/10.1038/s41467-020-18002-w | PubMed

Al Abed AS, Sellami A, Potier M, Ducourneau EG, Gerbeaud-Lassau P, Brayda-Bruno L, Lamothe V, Sans N, Desmedt A, Vanhoutte P, *et al.* (2020b) Age-related impairment of declarative memory: linking memorization of temporal associations to GluN2B redistribution in dorsal CA1. *Aging Cell* 1-12 https://doi.org/10.1111/acel.13243 | PubMed

Bal VH, Kim SH, Cheong D, Lord C (2015) Daily living skills in individuals with autism spectrum disorder from 2 to 21 years of age. *Autism* **19**:774-784 https://doi.org/10.1177/1362361315575840 | PubMed

Banker SM, Gu X, Schiller D, Foss-Feig JH (2021) Hippocampal contributions to social and cognitive deficits in autism spectrum disorder. *Trends in neurosciences* https://doi.org/10.1016/j.tins.2021.08.005 | PubMed

Barrientos SA, Tiznado V (2016) Hippocampal CA1 subregion as a context decoder. *Journal of Neuroscience* **36**:6602-6604 https://doi.org/10.1523/JNEUROSCI.1107-16.2016 | PubMed

Blanchard RJ, Flannelly KJ, Blanchard DC (1986) Defensive behavior of laboratory and wild Rattus norvegicus. *Journal of comparative psychology* **100**:101-107 https://doi.org/10.1037/0735-7036.100.2.101 | PubMed

Bowler D, Gaigg S, Lind S (2011) Memory in autism: Binding, self and brain. In: Roth I, Rezaie P (Eds). *Researching the Autism Spectrum: Contemporary Perspectives* Cambridge University Press. pp. 316-346 https://doi.org/10.1017/CBO9780511973918.013

Brewin CR (2011) The Nature and Significance of Memory Disturbance in Posttraumatic Stress Disorder. *Annu Rev Clin Psychol* **7**:203-203 https://doi.org/10.1146/ANNUREV-CLINPSY-032210-104544 | PubMed

Brunner D, Kabitzke P, He D, Cox K, Thiede L, Hanania T, Sabath E, Alexandrov V, Saxe M, Peles E, *et al.* (2015) Comprehensive Analysis of the 16p11.2 Deletion and Null Cntnap2 Mouse Models of Autism Spectrum Disorder. *PLOS One* **10**:e0134572 https://doi.org/10.1371/JOURNAL.PONE.0134572 | PubMed

Buonomano D V, Buzsáki G, Davachi L, Nobre AC (2023) Time for Memories. *Journal of Neuroscience* 7565-7574 https://doi.org/10.1523/JNEUROSCI.1430-23.2023 | PubMed

Buzsáki G, Tingley D (2018) Space and Time: The Hippocampus as a Sequence Generator. *Trends in Cognitive Sciences* https://doi.org/10.1016/j.tics.2018.07.006 | PubMed

Chang Q, Gold PE (2003) Switching memory systems during learning: changes in patterns of brain acetylcholine release in the hippocampus and striatum in rats. *The Journal of neuroscience : the official journal of the Society for Neuroscience* **23**:3001-5 PubMed | https://doi.org/10.1523/jneurosci.23-07-03001.2003

Chowdhury N, Quinn JJ, Fanselow MS (2005) Dorsal hippocampus involvement in trace fear conditioning with long, but not short, trace intervals in mice. *Behavioral Neuroscience* **119**:1396-1402 https://doi.org/10.1037/0735-7044.119.5.1396 | PubMed

American Psychiatric Association (2013) *Diagnostic and statistical manual of mental disorders : DSM-5* American Psychiatric Association Publishing.

Eichenbaum H (2014) Time cells in the hippocampus: a new dimension for mapping memories. *Nature Reviews Neuroscience* **15**:732-44 https://doi.org/10.1038/nrn3827 | PubMed

Eichenbaum H (2004) Hippocampus: Cognitive Processes and Neural Representations that Underlie Declarative Memory The hippocampus serves a critical role in declarative. *Neuron* **44**:109-120 https://doi.org/10.1016/j.neuron.2004.08.028 | PubMed

Etchamendy N, Desmedt A, Cortes-Torrea C, Marighetto A, Jaffard R (2003) Hippocampal lesions and discrimination performance of mice in the radial maze: sparing or impairment depending on the representational demands of the task. *Hippocampus* **13**:197-211 https://doi.org/10.1002/hipo.10055 | PubMed

Etchamendy N, Konishi K, Pike GB, Marighetto A, Bohbot D, Bohbot VD (2012) Evidence for a virtual human analog of a rodent relational memory task: a study of aging and fMRI in young adults. *Hippocampus* **22**:869-80 https://doi.org/10.1002/hipo.20948 | PubMed

Ferbinteanu J (2016) Contributions of hippocampus and striatum to memory-guided behavior depend on past experience. *Journal of Neuroscience* **36**:6459-6470 https://doi.org/10.1523/JNEUROSCI.0840-16.2016 | PubMed

Hollunder B, Ostrem JL, Sahin IA, Rajamani N, Oxenford S, Butenko K, Neudorfer C, Reinhardt P, Zvarova P, Polosan M, *et al.* (2024) Mapping dysfunctional circuits in the frontal cortex using deep brain stimulation. *Nature Neuroscience* **27**:573-586 https://doi.org/10.1038/s41593-024-01570-1 | PubMed

Hon OJ, Neira S, Flanigan ME, Roland A V, Caira CM, Sides T, D'Ambrosio SL, Lee SI, Simpson Y, Buccini MC, *et al.* (2025) Sex differences in BNST signaling and BNST CRF in fear processing. *eLife* **12** https://doi.org/10.7554/elife.89189 | PubMed

Leal SL, Yassa MA (2015) Neurocognitive Aging and the Hippocampus across Species. *Trends in Neurosciences* **38**:800-12 https://doi.org/10.1016/j.tins.2015.10.003 | PubMed

Maister L, Plaisted-Grant KC (2011) Time perception and its relationship to memory Autism Spectrum Conditions. *Developmental Science* **14**:1311-1322 https://doi.org/10.1111/j.1467-7687.2011.01077.x | PubMed

Marighetto A., Brayda-Bruno L., Etchamendy N (2011) Studying the Impact of Aging on Memory Systems: Contribution of Two Behavioral Models in the Mouse. In: Pardon MC., Bondi M. (Eds). *Behavioral Neurobiology of Aging. Current Topics in Behavioral Neurosciences* **10** Heidelberg: Springer, Berlin. https://doi.org/10.1007/7854_2011_151

Mingaud F, Le Moine C, Etchamendy N, Mormède C, Jaffard R, Marighetto A (2007) The hippocampus plays a critical role at encoding discontiguous events for subsequent declarative memory expression in mice. *Hippocampus* **17**:264-70 https://doi.org/10.1002/hipo.20262 | PubMed

Minor GN, Hannula DE, Gordon A, Ragland JD, Iosif AM, Solomon M (2023) Relational memory weakness in autism despite the use of a controlled encoding task. *Frontiers in Psychology* **14** https://doi.org/10.3389/fpsyg.2023.1210259 | PubMed

Mocle AJ, Ramsaran AI, Jacob AD, Rashid AJ, Luchetti A, Tran LM, Richards BA, Frankland PW, Josselyn SA (2024) Excitability mediates allocation of pre-configured ensembles to a hippocampal engram supporting contextual conditioned threat in mice. *Neuron* **112**:1487-1497.e6. https://doi.org/10.1016/J.NEURON.2024.02.007 | PubMed

Parkinson RG, Xu T, Martin J, Xian Z, Ziko I, Pettitt JA, RCom-H'Cheo-Forgues A, Buckland R, Gordon SL, Parish C, *et al.* (2024) Alpha-Synuclein Induced Immune Response Triggers Parkinson's Disease-Like Symptoms. *bioRxiv* 2024.05.27.596130 https://doi.org/10.1101/2024.05.27.596130

Paterno R, Marafiga JR, Ramsay H, Li T, Salvati KA, Baraban SC (2021) Hippocampal gamma and sharp-wave ripple oscillations are altered in a Cntnap2 mouse model of autism spectrum disorder. *Cell Reports* **37** https://doi.org/10.1016/j.celrep.2021.109970 | PubMed

Peñagarikano O, Abrahams BS, Herman EI, Winden KD, Gdalyahu A, Dong H, Sonnenblick LI, Gruver R, Almajano J, Bragin A, *et al.* (2011) Absence of CNTNAP2 leads to epilepsy, neuronal migration abnormalities, and core autism-related deficits. *Cell* **147**:235-46 https://doi.org/10.1016/j.cell.2011.08.040 | PubMed

Peñagarikano O, Geschwind DH (2012) What does CNTNAP2 reveal about autism spectrum disorder?. *Trends in Molecular Medicine* **18**:156-163 https://doi.org/10.1016/j.molmed.2012.01.003 | PubMed

Rashid AJ, Yan C, Mercaldo V, Hsiang H-L, Park S, Cole CJ, De Cristofaro A, Yu J, Ramakrishnan C, Lee SY, *et al.* (2016) Competition between engrams influences fear memory formation and recall. *Science* **353**:383-387 https://doi.org/10.1126/science.aaf0594 | PubMed

Ring M, Gaigg SB, Altgassen M, Barr P, Bowler DM (2018) Allocentric Versus Egocentric Spatial Memory in Adults with Autism Spectrum Disorder. *Journal of Autism and Developmental Disorders* **48**:2101 https://doi.org/10.1007/S10803-018-3465-5 | PubMed

Rumball F, Happé F, Grey N (2020) Experience of Trauma and PTSD Symptoms in Autistic Adults: Risk of PTSD Development Following DSM-5 and Non-DSM-5 Traumatic Life Events. *Autism Research* **13**:2122-2132 https://doi.org/10.1002/AUR.2306 | PubMed

Sellami A, Abed A, Brayda-Bruno L, Etchamendy N, Valério S, Oulé M, Pantaléon L, Lamothe V, Potier M, Bernard K, *et al.* (2018) Protocols to Study Declarative Memory Formation in Mice and Humans: Optogenetics and Translational Behavioral Approaches. *Bio-protocol* **8** https://doi.org/10.21769/BioProtoc.2888 | PubMed

Sellami A, Al Abed AS, Brayda-Bruno L, Etchamendy N, Valério S, Oulé M, Pantaléon L, Lamothe V, Potier M, Bernard K, *et al.* (2017) Temporal binding function of dorsal CA1 is critical for declarative memory formation. *Proceedings of the National Academy of Sciences of the United States of America* **114** https://doi.org/10.1073/pnas.1619657114 | PubMed

Simon DM, Wallace MT (2016) Dysfunction of sensory oscillations in Autism Spectrum Disorder. *Neuroscience and Biobehavioral Reviews* https://doi.org/10.1016/j.neubiorev.2016.07.016 | PubMed

Tsien JZ, Huerta PT, Tonegawa S (1996) The Essential Role of Hippocampal CA1 NMDA Receptor – Dependent Synaptic Plasticity in Spatial Memory. *Cell* **87**:1327-1338 https://doi.org/10.1016/s0092-8674(00)81827-9 | PubMed

Uddin LQ, Supekar K, Lynch CJ, Cheng KM, Odriozola P, Barth ME, Phillips J, Feinstein C, Abrams DA, Menon V (2015) Brain state differentiation and behavioral inflexibility in autism. *Cerebral Cortex* **25**:4740-4747 https://doi.org/10.1093/cercor/bhu161 | PubMed

Van Wijngaarden-Cremers PJM, Van Eeten E, Groen WB, Van Deurzen PA, Oosterling IJ, Van Der Gaag RJ (2014) Gender and age differences in the core triad of impairments in autism spectrum disorders: a systematic review and meta-analysis. *Journal of autism and developmental disorders* **44**:627-635 https://doi.org/10.1007/S10803-013-1913-9 | PubMed

Vogel DHV, Jording M, Esser C, Conrad A, Weiss PH, Vogeley K (2022) Temporal binding of social events less pronounced in individuals with Autism Spectrum Disorder. *Scientific Reports* **12** https://doi.org/10.1038/s41598-022-19309-y | PubMed

Wang J, Christensen D, Coombes SA, Wang Z (2024) Cognitive and brain morphological deviations in middle-to-old aged autistic adults: A systematic review and meta-analysis. *Neuroscience and Biobehavioral Reviews* https://doi.org/10.1016/j.neubiorev.2024.105782 | PubMed

White NM, McDonald RJ (2002) Multiple parallel memory systems in the brain of the rat. *Neurobiology of learning and memory* **77**:125-84 https://doi.org/10.1006/nlme.2001.4008 | PubMed

Zhang L, Chen P, Schafer M, Zheng S, Chen L, Wang S, Liang Q, Qi Q, Zhang Y, Huang R (2022) A specific brain network for a social map in the human brain. *Scientific Reports* **12** https://doi.org/10.1038/s41598-022-05601-4 | PubMed

Peer reviews

Reviewer #1 (Public review):

Summary:

The uniqueness of this paper is the study of the formation of temporal binding-dependent memories in the cntnap2 mouse, a long-standing mouse model of autism that has been used to test therapeutic modalities.

Strengths:

I liked the combination of optical recordings and interventions and the backup of primary observations with control experiments.

Weaknesses:

(1) Fiber photometry recordings are too coarse to give salient clues to the underlying mechanism.

(2) Are perturbed pyramidal cells causally responsible for the altered trace? What can be concluded about the possible role of inhibitory interneurons as potential drivers? The observations focus on abnormal regional activity as observed with fiber photometry and manipulated by optogenetics. The authors should state clearly the limits of their conclusions.

(3) I found the "trace" nomenclature confusing. "....in which mice are required to memorize the association between a tone (Conditioned Stimulus) and a mild electric foot-shock (Unconditioned Stimulus), separated by a time interval called Trace (Sellami et al., 2017)." It seems that the conceptual model invokes the creation of an [eligibility] trace, characterized by its progressive disappearance over time. It may be a convention in the field or a matter of language, but it seems perverse to use "trace" to label the time interval rather than the entity that is decaying. If this is an accepted convention going back to Howard Eichenbaum, the authors should cite the paper that first introduced the convention.

(4) I would advocate for the addition of some discussion points for the authors to consider.

a) Is the retention of activity in CA1 related to phenomena at the cellular or subcellular level in CA1 pyramidal cells? I'm thinking of dendritic, delayed, and stochastic CaMKII activation (DDSC) as defined by Yasuda's group or short-term and associative plasticity of calcium dynamics (STAPCD) as delineated by Caya-Bissonette and Beique.

b) Was the optogenetic intervention ever administered in a delayed fashion, capitalizing on the temporal advantages of optogenetics to probe dynamics?

c) Is the newfound reliance on corticostriatal pathways something more than compensation at the behavioral level? Could it be driven in part by the ASD-related genetic changes?

https://doi.org/10.7554/eLife.111851.1.sa2

Reviewer #2 (Public review):

The authors investigate the contribution of dorsal CA1 hippocampal dysfunction to cognitive impairments in the Cntnap2 knockout mouse model of autism spectrum disorder. Building on previous evidence implicating the hippocampus in episodic and relational memory processes, they combine trace fear conditioning, fiber photometry, optogenetic manipulation, a relational/declarative memory radial maze task, and cFos mapping to test whether altered CA1 function contributes to deficits in temporal binding and memory flexibility.

The study has several important strengths. First, the work addresses a relatively understudied aspect of autism-related cognition, namely hippocampal-dependent memory processes, whereas much of the literature has focused on social behavior, cortical circuits, or striatal dysfunction. Second, the authors employ multiple complementary approaches that converge on a coherent mechanistic hypothesis. The behavioral data demonstrate a reduced ability of Cntnap2 knockout mice to retain associations across long temporal gaps. Fiber photometry recordings reveal reduced dorsal CA1 activity during conditions that challenge temporal binding, and optogenetic activation of dorsal CA1 neurons during the trace interval is sufficient to rescue memory performance. Together, these findings provide strong support for a causal contribution of dorsal CA1 activity to temporal binding deficits in this model.

The second major strength of the manuscript is the extension of these findings to a more complex hippocampus-dependent memory task. The radial maze experiments indicate that Cntnap2 knockout mice show impaired memory flexibility and a greater reliance on egocentric learning strategies. The accompanying cFos analyses suggest altered recruitment

of hippocampal and striatal networks during learning, providing a systems-level framework that may explain the observed behavioral phenotype.

Overall, the main conclusions regarding impaired temporal binding and reduced dorsal CA1 engagement are well supported by the data. The optogenetic rescue experiments are particularly compelling because they move beyond correlation and directly test causality. The manuscript therefore makes a meaningful contribution to our understanding of how hippocampal dysfunction may contribute to cognitive abnormalities associated with autism.

Weaknesses:

Some conclusions are necessarily more inferential than others. In particular, the interpretation that the observed behavioral phenotype reflects a broader shift from hippocampal-dependent declarative memory toward striatum-dependent procedural learning is supported primarily by cFos activity patterns and behavioral strategy measures. While the data are consistent with this interpretation, they do not directly demonstrate a causal reorganization of memory systems. Similarly, although the findings identify a mechanism in the Cntnap2 model, caution is warranted when extrapolating these conclusions to autism spectrum disorder more broadly; but I believe this caution is addressed in the discussion.

Despite these limitations, the study presents a coherent and well-executed body of work that provides novel mechanistic insight into hippocampal contributions to cognitive dysfunction in a widely used autism model. The findings should be of considerable interest to researchers studying hippocampal function, memory systems, and neurodevelopmental disorders.

https://doi.org/10.7554/eLife.111851.1.sa1

Reviewer #3 (Public review):

Summary:

The manuscript evaluated behavioral phenotypes in the Cntnap2 knockout mouse using two behavioral paradigms: trace fear conditioning and a radial maze task. The trace fear conditioning training is normal, but memory generalization is impaired. The inflexibility is suggested to be related to low activity in dCA1 neurons, which can be rescued by ChR2. The radial maze task data suggested a similar conclusion. Brain-wide cFos mapping indicated impairments in the Cntnap2 knockout mouse. The brain-wide cFos mapping does not show direct correlations with Cntnap2, limiting the interpretation of these data in the context of this paper.

Strengths:

The behavior data are solid.

Weaknesses:

The underlying mechanism is not fully investigated.

Major points：

(1) The authors should thoroughly check their manuscript as there are many typos in the current version that affect the readability.

(2) In trace fear conditioning, the tone test impairment can be rescued by ChR2. Have the authors tried rescue experiments with Cntnap2? Rescue experiments in the radial maze task are also essential, either with ChR2 or Cntnap2.

(3) The quality of the cFos example image in Figure 3 is too low. The authors should also provide example images for the other brain regions in the supplementary data, if possible.

(4) The causal link between the brain-wide cFos mapping and the Cntnap2 knockout is weak. How to explain the increase of cFos cell densities in some brain regions, but the decrease in others?

https://doi.org/10.7554/eLife.111851.1.sa0